

## **RAIN ATTENUATION PREDICTIONS AT KU-BAND IN SOUTH EAST ASIA COUNTRIES**

**J. S. Mandeep**

School of Electrical and Electronic Engineering  
University Sains Malaysia  
Engineering Campus, 14300 Nibong Tebal  
Seberang Perai Selatan, Penang, Malaysia

**J. E. Allnut**

Department of Electrical and Computing Engineering  
George Mason University  
4400 University Drive, Virginia, USA

**Abstract**—The rain attenuation in the 12-GHz band and one-minute-rain rate were measured at four satellite beacons located in South East Asia countries over a three-year period (2002–2004). The cumulative distribution of rain rate obtained as well as cumulative distribution of rain attenuation obtained are presented and compared with the rain prediction models. Most of the rain prediction models showed noticeable deviation to the measured values above the existence of the breakpoint (the point at which the slope changes). The results can be employed to guide the design and application of slant-path communication systems, especially in South East Asia countries.

### **1. INTRODUCTION**

Rain attenuation is by far the most important of losses for frequencies above 10 GHz, because it can cause the largest attenuation and is usually, therefore, the limiting factor at Ku-band satellite link design [1]. Rain rate distribution is one of the most important factors for calculating rainfall attenuation at a specific location. The most effective way of obtaining the cumulative rainfall distribution is through direct measurement. However due to the shortage of the required rainfall data at certain locations, rainfall models need to be

introduced to predict the rainfall rate and attenuation distribution at location of interest [2–4].

Attenuation by rain can be predicted accurately if the rain is precisely described all the way along the path [5]. Path attenuation is essentially an integral of all individual increments of rain attenuation caused by the drops encountered along the path [6, 7]. This is physical approach to predict rain attenuation. Unfortunately, rain cannot be described accurately along the path without extensive meteorological database, which does not exist in most regions of the world [1]. Most prediction models therefore resort to semi empirical approaches. The semi empirical approach is based on two factors, firstly the rainfall rate at a point on the surface of the earth is statically related (over a period of at least a year) to the attenuation encountered along the path to a satellite and secondly the actual path length of the path through the rain medium can be adjusted in such a way that the *effective path length*,  $L_{eff}$  is developed over which the rain can be considered to be homogeneous [8].

Over the past several years extensive efforts have been undertaken to develop reliable techniques for the prediction of path rain attenuation for a given location and frequency, and the availability of satellite beacon measurements has provided a database for the validation and refinement of the predictions models [9, 10]. Most of these rain attenuation models that has been developed by researches was based on the data collected from temperate regions [11]. Rain in these regions is mostly of stratiform structure, which is generally ‘light’ with relatively large rain cell diameters. However, in the tropics, rain at times is from convective rain cells, with relatively small diameter [12] often resulting in ‘heavy’ down pours for short periods [13]. The precipitation observed over the globe often are a combination of the two rather than simply one or the other, however, the frequency of a particular rain structure may dominate a region [14]. In temperate climates, due to the large rain cell diameter, the attenuation increases with decrease in the elevation angle, however in the tropics, for the same rain rate, the converse is found to be true [15].

In this paper, we compare the results of rain rate and attenuation study on Ku-band satellite link in a tropical site with some of the available models for the region. The exceedance curves for rain rate and attenuation showed clear breakpoint (the trend of variation of the slope of the curve changes suddenly) implying changes in the rain structure and attenuation.

## 2. METHODOLOGY

The experimental site was the University Sains Malaysia (USM), Institute Technology Bandung (ITB), Ateneo de Manila University (AdMU), and University of South Pacific (USP). Descriptions of the measurement site are presented in Table 1. The receiver antennas are pointed towards JCSAT-1B located at  $128^\circ\text{E}$  for ITB, INTELSAT 701 located at  $180^\circ\text{E}$  for USP and SUPERBIRD-C located at  $144^\circ\text{E}$  for USM and AdMU. The SUPERBIRD-C, JCSAT-1B and INTELSAT 701 are highly reliable three-axis stabilized spacecraft with a transponder RF output power of 90, 60 and 120 W, respectively at Ku-Band.

**Table 1.** Measurement sites characteristics.

Measurement Site	USM	ITB	AdMU	USP
Earth station location	$5.17^\circ\text{N}$ $100.4^\circ\text{E}$	$6.5^\circ\text{S}$ $107.4^\circ\text{E}$	$14.7^\circ\text{N}$ $121.1^\circ\text{E}$	$18.1^\circ\text{S}$ $178.3^\circ\text{E}$
Beacon frequency (GHz)	12.255	12.247	12.255	11.610
Antenna elevation (deg)	$40.1^\circ$	$64.7^\circ$	$58.8^\circ$	$68.7^\circ$
Altitude (m)	57	700	80	20
Antenna diameter (m)	2.4	1.8	1.8	1.2
Equipment outage time in year 1	99%	99.2%	99.6%	98.9%
Equipment outage time in year 2	99.4%	99%	98%	98.5%
Equipment outage time in year 3	98%	99.8%	99.2%	99.4%

The beacon measurement was taken through a signal transmitted from the operational transponder. The orientation of the receiver antennas is horizontal polarized. The output signal of the LNB, at the dish, was connected to a data logger via personnel computer (PC) at USM, ITB and AdMU whereas at USP, was connected to a spectrum analyzer, which was interface to a computer via a labVIEW interfacing card [12]. For all measurement sites labVIEW software was used and programmed to record the peaks of sixty successive samples each of 1 ms duration. The software then calculates the mean of these sixty peak values. These recordings were then repeated every 10 s giving six averaged peak values in a minute. To account for any variation in the satellite signal strength due to orbital variations, the average clear day signal strengths on the day prior to and after the rainy day(s) were used in the computation of the rain attenuation [12].

The rain rate was measured using a tipping bucket arrangement of diameter 20-cm with a calibration of 0.2 mm of rainfall per tip at USP whereas at USM, ITB and AdMU calibration of 0.5 mm of rainfall per tip was used. The rain gauges has its own programmable data logger which records the time of each tip to an accuracy of 0.1 s. The clock of the logger was regularly synchronized with that of the computer. The availability of the instruments reached 99% of the total observation time. The 1% of unavailability (about 262 hours in the 36-month period) is built up by 130 outage events, most of them with duration of less than two hours, during which the equipments was out of function, most likely due to electric power failure and calibration of equipments. Among the total of 130 outage events, only 10 occurred in between light rain event. The rain gauge and beacon receiver did not miss out any heavy rain event. The outage time is the average of the four measurement sites.

### 3. RESULTS AND DISCUSSION

The cumulative distributions of rain rate and attenuation at measured sites are shown in Figs. 1 and 2, respectively. For all of the four measurement sites, the rain attenuation values are almost the same from 1% to 0.1% percentage of time. The rain attenuation deviates from 0.01% to 0.001% percentage of time. This is due to the heavy rainfall events at each measurement site. The measurements of rain rate are mostly convective in the measurement site except at USP. Therefore there is not much of difference in the rain attenuation values for higher percentage of time at USM, ITB and AdMU. If the rain rate is stratiform then there will be difference of more than 25% in dB for the higher percentage of time from 1% to 0.1%.

The exceedance curves in Fig. 1, shows that as the rain rate increases, the trend of the slope curve gradually decreases from a large negative value, and then the trend is reversed. The point at which the trend changes is referred to as the 'breakpoint' in the exceedance curves [4, 16]. In Figs. 1 and 2 an arrow denotes the breakpoint. The breakpoint in the exceedance curves usually occurs at high rain rates. When the rain structure is stratiform, rainfall is widespread, with low rain rates. In the tropics, however when the cloud builds up, the water droplets are caught in updrafts inside the cloud and are vertically transported. This enhances the coalescence of water particles, resulting in convective heavy rain [17]. Thus any change in the trend of the slope of the exceedance curves, as shown by the breakpoint, signifies that rain structure changes from stratiform at low rain rates to mostly convective at high rain rates.

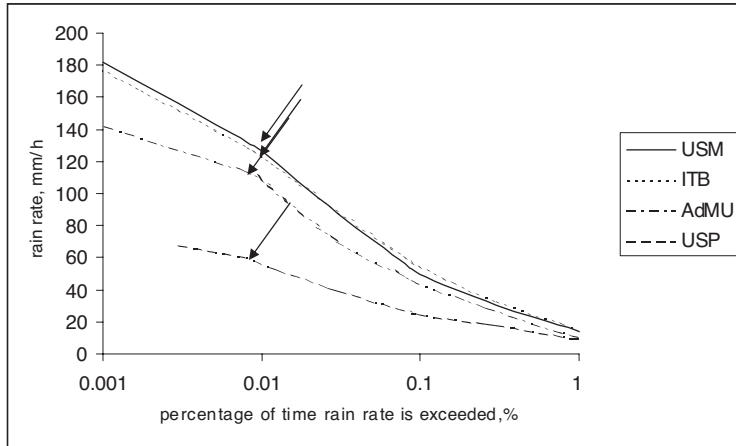


Figure 1. Cumulative distribution of measured rain rate.

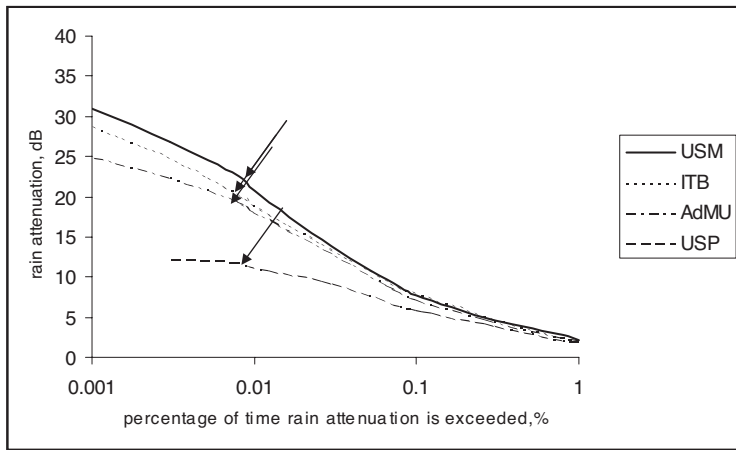
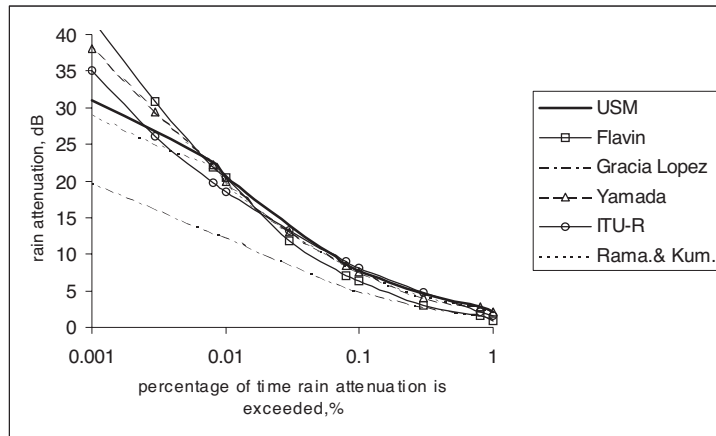


Figure 2. Cumulative distribution of measured rain attenuation.

#### 4. COMPARISONS OF PREDICTION MODELS

The cumulative distributions of the measured rain attenuation were compared with five tropical regions prediction models known as [18–22] and [12]. Fig. 3 to Fig. 6 shows the comparisons. The Gracia-Lopez model underestimates the measured rain attenuation values for all the measurement sites throughout the entire percentage of time where rain attenuation is exceeded. This is because model was



**Figure 3.** Comparison of measured and predicted attenuation distributions — USM.

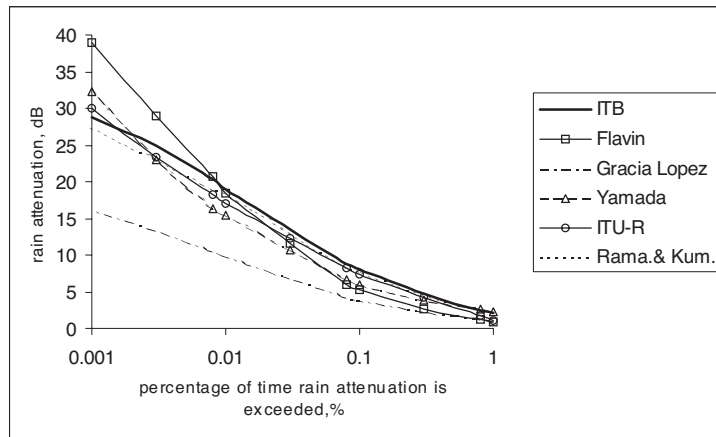


**Figure 4.** Comparison of measured and predicted attenuation distributions — ITB.

developed based on low rain rate intensity (reaching up to 60 mm/h at 0.003% of time rain rate us exceeded) in satellite links having low elevation angle below  $30^\circ$ . Moreover, the model assumed that the specific attenuation is constant from the ground up to the melting layer ( $0^\circ\text{C}$  isotherm height). The Ramachandran and Kumar model follows closely the measured rain attenuation values for all the measurement sites throughout the entire percentage of time where rain attenuation

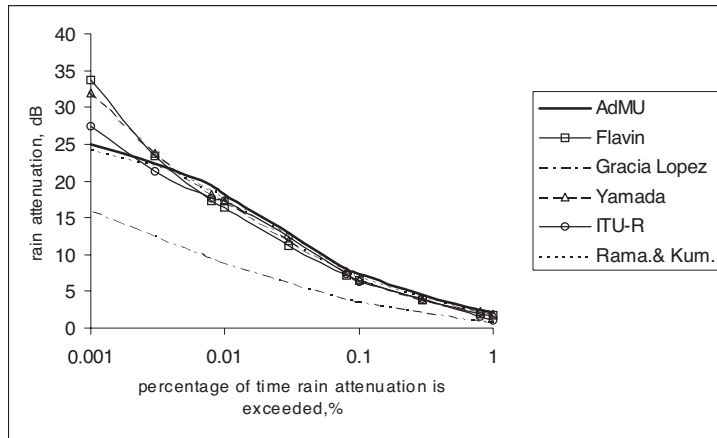


**Figure 5.** Comparison of measured and predicted attenuation distributions — AdMU.

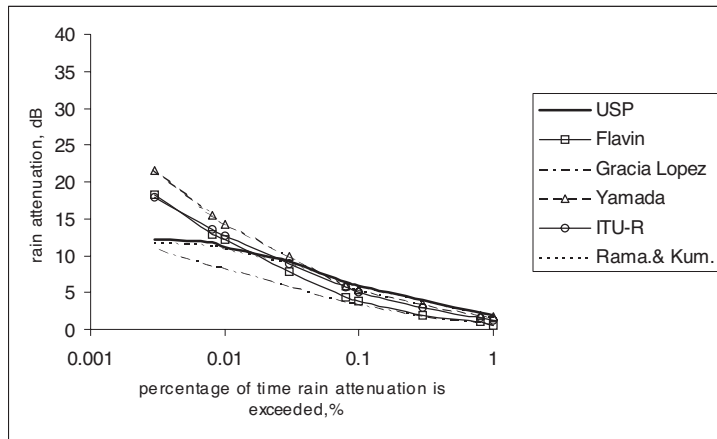


**Figure 6.** Comparison of measured and predicted attenuation distributions — USP.

is exceeded. The model introduced a correction factor to calculate the attenuation for paths with elevation angle  $<70^\circ$ . This is to accommodate a margin error in the estimate of the rain cell diameters in the tropics. This may be due to the fact that, at low elevation angles, the incoming signal beam intercepts more than one rain cell. The Flavin model underestimates the measured rain attenuation values from 1% to 0.01% before overestimating the measured values from

0.01% to 0.001% of time rain attenuation is exceeded. The model shows a monotonous decrease. The model is based on relevant ITU-R information of rain cell size and height of the 0°C isotherm, and no other parameters were used to minimize the prediction errors. The model used too few rain climate zones to span the wide range of rain conditions present in the tropical region. The Yamada model follows closely to the measured rain attenuation values from 1% to 0.01% of time rain attenuation is exceeded at USM, AdMU and USP. The model tends to overestimate these measurement sites from 0.01% to 0.001% of time. At ITB the model underestimates the measured values from 1% to 0.003% of time the rain attenuation is exceeded. This is due to the fact that the use vertical path reduction coefficient for the models that employ a direct calculation of the attenuation value that calculate the probability of exceeding the specified attenuation was not considered. The model assumes a universal shape for attenuation cumulative distribution so all that is required is the estimation of the rain rate, path length and path reduction factor at a single probability level. The ITU-R model agrees reasonably well with the measured values, however the attenuation predicted deviates considerably from the measured values at higher rain rates from 0.01% to 0.001% of time rain attenuation is exceeded for all measurement sites. One of the dominant features of the experimental values is the saturation of attenuation, which can be caused by saturation of rain at very high rain rate. As the rain rate increases, reaching a maximum of 10 km while the rain cell diameter continues to decrease. Therefore, the proportional increase of rain volume, which is a function of rain rate, rain cell diameter and rain column height, would be saturating [7, 15].

## 5. CONCLUSION

A significant feature of rain rate and attenuation exceedance curves in the tropical region is the occurrence of the breakpoint. In the tropics, it was found that at medium to low rain rates, the models agree reasonably well with the measured attenuation values and tend to deviate at higher rain rates. The proposed model by Ramachandran and Kumar, using breakpoints, proved to be a success in predicting the attenuation exceedance in the tropical region.

## ACKNOWLEDGMENT

The author would like to acknowledge the University Research Committee and Association Radio Industries Business of Japan (ARIB) for supporting this work.



## REFERENCES

1. Timothy, P., W. C. Bostian, and J. E. Allnutt, *Satellite Communication*, 2nd edition, John Wiley & Sons, 2003.
2. Mandeep, J. S. and S. I. S. Hassan, "Comparison of 1-minute rainfall rate distribution for tropical and equatorial climates," *Space Communication*, Vol. 19, 193–198, IOS Press, 2004.
3. Panagopoulos, A. D. and J. D. Kanellopoulos, "On the rain attenuation dynamics: spatial-temporal analysis of rainfall rate and fade duration statistics," *International Journal of Communications and Networking*, Vol. 21, No. 6, 595–611, 2003.
4. Bryant, G. H., I. Adimula, C. Riva, and G. Brussard, "Rain attenuation statistics from rain column diameters and heights," *International Journal of Satellite Communications*, Vol. 19, No. 3, 263–283, 2001.
5. Ramachandran, V. and V. Kumar, "Invariance of accumulation time factor of ku-band signals in the tropics," *Journal of Electromagnetic Waves and Applications*, Vol. 19, No. 11, 1501–1509, 2005.
6. Matricciani, E., "Service oriented statistics of interruption time due to rainfall in earth-space communication systems," *IEEE Transaction on Antennas and Propagation*, Vol. 52, No. 8, 2083–2090, 2004.
7. Kumar, V. and V. Ramachandaran, "Rain attenuation measurement at 11.6 GHz in Suva, Fiji," *Electronic Letters*, Vol. 40, No. 2, 1429–1431, 2004.
8. Panagopoulos, A. D. and G. E. Chatzarakis, "Outage performance of single/dual polarized fixed wireless access links in heavy rain climatic regions," *Journal of Electromagnetic Waves and Applications*, Vol. 21, No. 3, 283–297, 2007.
9. Tseng, C. -H., K. -S. Chen, J. C. Shi, and C. H. Chu, "Prediction of Ka-band terrestrial rain attenuation using 2-year rain drop size distribution measurements in Northern Taiwan," *Journal of Electromagnetic Waves and Applications*, Vol. 19, No. 13, 1833–1841, 2005.
10. Li, Y. and P. Yang, "The permittivity based on electromagnetic wave attenuation for rain medium and its applications," *Journal of Electromagnetic Waves and Applications*, Vol. 20, No. 15, 2231–2238, 2006.
11. Singh, M. S. J., S. I. S. Hassan, M. F. Ain, K. Igarashi, K. Tanaka, and M. Iida, "Rain attenuation model for S. E. Asia countries," *IET Electronic Letters*, Vol. 43, No. 2, 75–77, 2007.

12. Ramachandaran, V. and V. Kumar, "Modified rain attenuation model for tropical regions for Ku-band signals," *International Journal of Satellite Communications and Networking*, Vol. 25, No. 1, 53–67, 2006.
13. Georgiadou, E. M., A. D. Panagopoulos, and J. D. Kanellopoulos, "Millimeter wave pulse propagation through distorted raindrops for LOS fixed wireless access channels," *Journal of Electromagnetic Waves and Applications*, Vol. 20, No. 9, 1235–1248, 2006.
14. Pan, Q. W. and J. E. Allnut, "12 GHz fade durations and intervals in the tropics," *IEEE Transaction on Antenna and Propagation*, Vol. 52, No. 3, 693–701, 2004.
15. Pan, Q. W., G. H. Bryant, J. McMahon, J. E. Allnut, and F. Haidara, "High elevation angle satellite to earth 12 GHz propagation measurements in the tropics," *International Journal of Satellite Communications*, Vol. 19, No. 4, 363–384, 2001.
16. Kumar, V., R. C. Deo, and V. Ramachandran, "Total rain accumulation and rain rate analysis for small tropical Pacific islands: a case study of Suva, Fiji," *Atmospheric Science Letters*, Vol. 7, 53–58, 2006.
17. Schumacher, C. and R. A. Houze, "Stratiform rain in the tropics as seen by TRMM precipitation radar," *American Meteorological Society*, Vol. 16, 1739–1756, 2003.
18. Flavin, R. K., "Rain attenuation considerations for satellite paths in Australia," *Australian Telecomm. Research*, Vol. 23, No. 2, 47–55, 1982.
19. Garcia, P. and M. L. A. R. Selvo, "Improved method for prediction of rain attenuation in terrestrial links," *Electronic Letters*, Vol. 40, No. 11, 683–684, 2004.
20. Yamada, M., Y. Karasawa, and M. Yasunaga, "An improved prediction method for rain attenuation in satellite communication operating at 10–20 GHz," *Radio Science*, Vol. 22, 1053–1062, 1987.
21. International Telecommunication Union (ITU-R), "Characteristics of precipitation for propagation modeling," Recommendation P.837-4, 2003.
22. International Telecommunication Union (ITU-R), "Propagation data and prediction methods required for the design of earth-space telecommunication systems," Recommendation P.618-8, 2003.